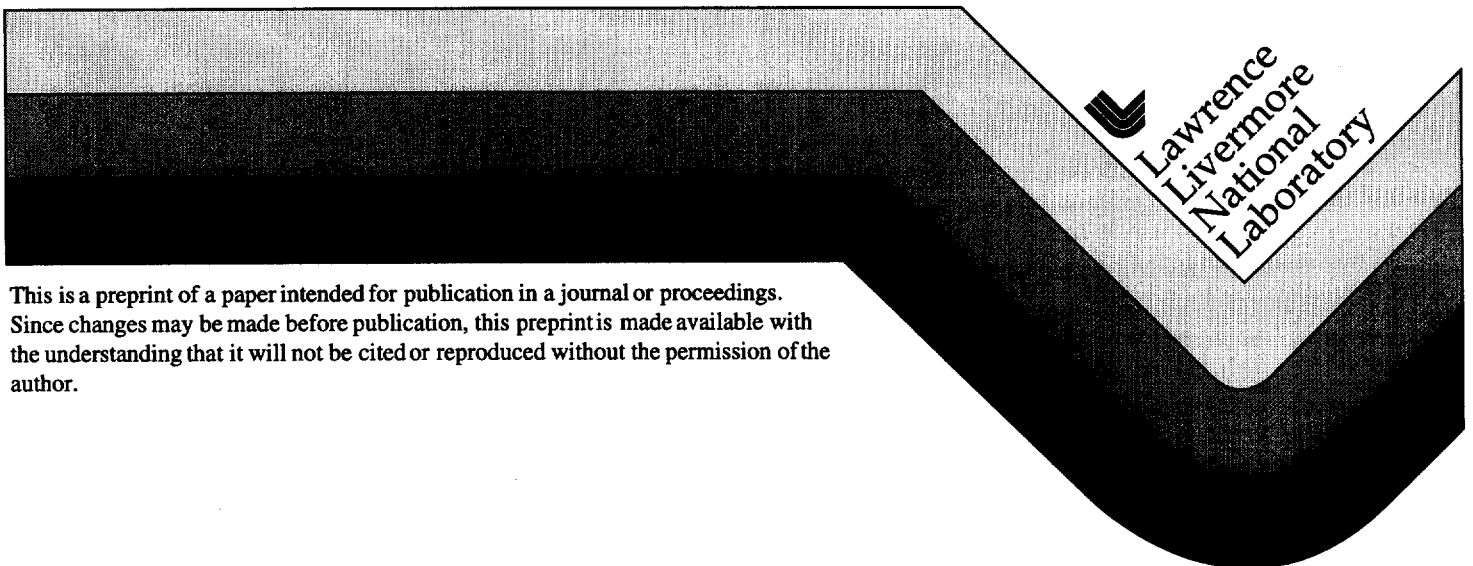


UCRL-JC-127579
PREPRINT

A New Meteorological Data Assimilation Model for Real-Time Emergency Response

This paper was prepared for submittal to the
*10th Joint Conference on the
Applications of Air Pollution Meteorology with the Air and Waste Management Association
Phoenix, AZ
January 11-16, 1998*

September 1997



This is a preprint of a paper intended for publication in a journal or proceedings. Since changes may be made before publication, this preprint is made available with the understanding that it will not be cited or reproduced without the permission of the author.

DISCLAIMER

This document was prepared as an account of work sponsored by an agency of the United States Government. Neither the United States Government nor the University of California nor any of their employees, makes any warranty, express or implied, or assumes any legal liability or responsibility for the accuracy, completeness, or usefulness of any information, apparatus, product, or process disclosed, or represents that its use would not infringe privately owned rights. Reference herein to any specific commercial product, process, or service by trade name, trademark, manufacturer, or otherwise, does not necessarily constitute or imply its endorsement, recommendation, or favoring by the United States Government or the University of California. The views and opinions of authors expressed herein do not necessarily state or reflect those of the United States Government or the University of California, and shall not be used for advertising or product endorsement purposes.

G. Sugiyama * and S. T. Chan

Lawrence Livermore National Laboratory, Livermore CA

1. INTRODUCTION

We are developing a new meteorological data assimilation model for the Atmospheric Release Advisory Capability (ARAC) project at Lawrence Livermore National Laboratory, which provides real-time dose assessments of airborne pollutant releases. The model, ADAPT (Atmospheric Data Assimilation and Parameterization Techniques), builds three-dimensional meteorological fields, which can be used to drive dispersion models or to initialize or evaluate mesoscale models. ADAPT incorporates many new features and substantial improvements over the current ARAC operational models MEDIC/MATHEW (ARAC, 1997), including the use of continuous-terrain variable-resolution grids, the ability to treat assorted meteorological data such as temperatures, pressure, and relative humidity, and a new algorithm to produce mass-consistent wind fields. In this paper, we will describe the main features of the model, current work on a new atmospheric stability parameterization, and show example results.

2. METEOROLOGICAL DATA

ADAPT uses input derived from ARAC's land-surface and real-time meteorological databases, archived experimental data sets, and analytically generated data. Local meteorological observations are currently provided to ARAC by the Air Force Global Weather Center, Domestic Data Plus, International Data Service, and supported site towers. Gridded analyses and forecast fields are obtained from the Fleet Numerical Meteorological and Oceanographic Center (NOGAPS model), the National Weather Service (AVN and ETA models), and ARAC adaptations of the mesoscale models NORAPS and COAMPS developed by the Naval Research Laboratory (Hodur, 1987 and 1997). Meteorological data is selected for a spatial region that is usually larger than the domain of the model simulations in order to use the most complete set of information relevant to the problem.

*Corresponding author address: G. Sugiyama, L-103, P. O. Box 808, Lawrence Livermore National Laboratory, Livermore, CA 94550; email sugiyama@llnl.gov

3. COMPUTATIONAL GRID

The model represents the ground surface by a piecewise bilinear interpolation of grid-point topographical data. Run-time selection of both the number of grid points and the grid resolution is provided, along with variable resolution in both the vertical and horizontal coordinates. The former permits a good representation of the meteorological fields in the critical near-surface region, while the latter is utilized when warranted by either topographical variation or data density. For the examples shown in this paper, the vertical coordinate is taken to be $\sigma_z = \frac{z-z_g}{z_{top}-z_g}$, where z_g is the ground elevation and z_{top} is the height of the grid top, the coordinate used by COAMPS and ARAC's new dispersion model LODI (Leone et al., 1997).

4. DATA ASSIMILATION

Diverse data assimilation techniques are being developed to meet the needs of a new generation of ARAC models and to take advantage of the rapidly expanding availability of meteorological and land-surface data. ADAPT provides a number of split methods, which perform separate vertical and horizontal analyses. Fully three-dimensional analysis are under development. Additional features include the incorporation of map projections and the treatment of atmospheric and land-surface parameters as spatially varying fields.

The vertical analysis is based on an idealized picture of the atmosphere as divided into a set of layers - the surface layer, the boundary layer, and the free atmosphere. Different interpolation methods and empirical parameterizations are then used in each layer, depending on atmospheric conditions. Several techniques are provided to coherently blend surface and tower data with upper air data and control the use of upper air data depending on their representativeness in time and space.

A variety of interpolation and extrapolation techniques are available in ADAPT. The simplest class of techniques is based on direct interpolation

$$\phi(\vec{r}, t) = \sum_k w_k(\vec{r}, t, \vec{r}_k, t_k) \phi_k \quad (1)$$

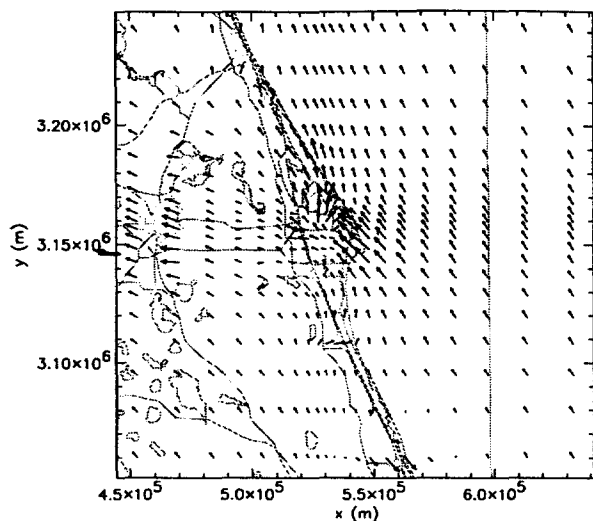


Figure 1: Cape Canaveral winds at 9 m AGL generated from observational data. Every third wind vector is plotted. The greatest wind speed shown is 3.7 m/s.

where ϕ_k are observations located at (\vec{r}_k, t_k) and w_k are normalized weights. The weights are typically monotonically decreasing functions of spatial distance or relative time. A large variety of algorithms are possible, based on different choices of the weighting functions. Examples include bilinear interpolation and methods based on inverse horizontal distance squared, inverse relative height, exponential time difference, and influence radius weighting. Specification of a maximum cutoff distance provides an additional means of controlling the weighting of the interpolation.

A second group of algorithms uses the method of successive corrections (Daley, 1991), which may be written schematically as

$$f_A^{j+1}(\vec{r}, t) = f_A^j(\vec{r}, t) + \sum_k w_k^j [f_o(\vec{r}_k) - f_A^j(\vec{r}_k)] \quad (2)$$

where f_A^j is the analyzed field at (\vec{r}, t) for the j^{th} iteration, $f_o(\vec{r}_k)$ is the k^{th} observation, and w_k^j are normalized weights. The weights can be altered with each iteration to act as filters for the removal of small scale noise or errors. One such method implemented in ADAPT is the Barnes algorithm for which $w(\vec{r}) = \exp(-\frac{\vec{r}^2}{2\bar{R}^2})$, with \bar{R} being a varying horizontal influence radius parameter.

5. EXAMPLE : CAPE CANAVERAL

As an example, ADAPT was used to generate wind fields for a site surrounding Cape Canaveral in Florida. The graded grid covers a region 180 km square with a grid top at 4.5 km using 61 grid points in the horizontal

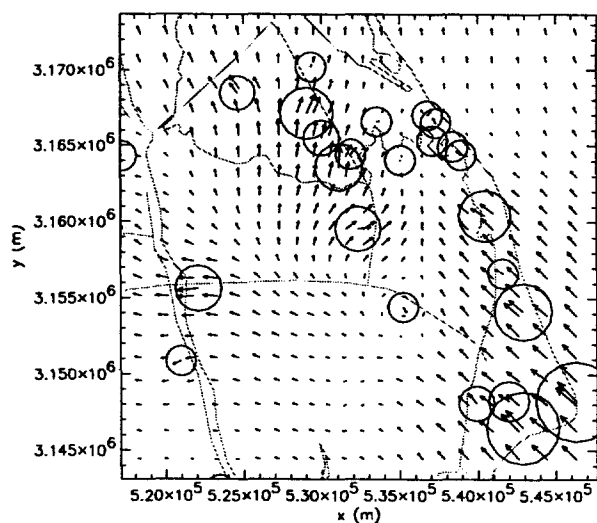


Figure 2: Enlargement of the wind field from the previous figure. Every wind vector is plotted. The vectors enclosed in circles are the observational data.

and 41 in the vertical. Figure 1 shows the 9 m above ground level (AGL) wind field for September 23, 1997 at 9Z. The field was developed from 49 surface and tower stations and 5 upper air profiles using an inverse-distance squared sparse data algorithm. Some of the observational data may be seen in the enlargement plotted in Figure 2, the plotted observational level being the one nearest in height to 9 m AGL. Complex wind structure is developed near the site where the meteorological data is dense.

Figure 3 plots the winds at the 9 m AGL level, derived from a NORAPS forecast for the same time, using a bilinear-linear analysis. This wind field shows a pattern reasonably similar to that in Figure 1, with a generally onshore flow, veering to the north near the site and accelerating to the west near the left hand side of the grid. However the speeds are significantly higher than indicated by the observations.

6. MASS-CONSISTENT WIND ADJUSTMENT

The generation of wind fields involves a few special considerations. Interpolation and parameterization may be performed in either speed and direction or u and v components. The inclusion of map projections requires appropriate adjustments of length scales and directions. The vertical wind component can be determined in the same fashion as the horizontal components if w data is available. However, this is generally not the case. Further, our applications typically require the wind field to be non-divergent, a property which is not *a priori* guaranteed by the interpolation methods. An adjustment pro-

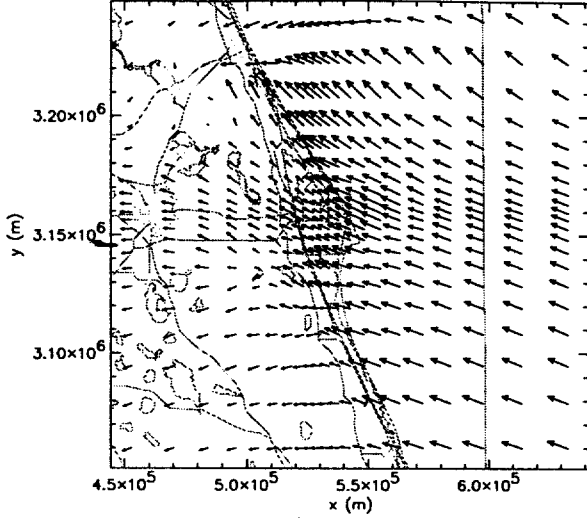


Figure 3: Cape Canaveral winds at 9 m AGL generated from a NORAPS forecast for the same time as in Figure 1. Every third vector is plotted. The largest vector shown is 6.8 m/s.

cedure based on the variational principle is therefore performed to provide the vertical wind component and produce mass-consistent winds.

ADAPT's mass-consistent wind algorithm (Chan and Sugiyama, 1997a and 1997b) is based on the following mixed variational principle

$$I(u, v, w, \lambda) = \frac{1}{2} \int_{\Omega} [\alpha_H^2 (u - u^o)^2 + \alpha_H^2 (v - v^o)^2 + \alpha_V^2 (w - w^o)^2] d\Omega + \int_{\Omega} \lambda \left(\frac{\partial u}{\partial x} + \frac{\partial v}{\partial y} + \frac{\partial w}{\partial z} \right) d\Omega \quad (3)$$

where (u^o, v^o, w^o) and (u, v, w) are the components of the initial and adjusted wind velocity fields, respectively, $\lambda(x, y, z)$ is the Lagrange multiplier for the mass-consistency constraint, α_H and α_V are the Gauss precision moduli controlling the vertical and horizontal velocity adjustments, and Ω is the domain.

The finite element method (FEM) is chosen for spatial discretization because of its effectiveness in treating complex terrain and its flexibility in dealing with variable resolution grids. In addition, the grid-point representation of the wind fields by FEM offers a more rigorous treatment of boundary conditions than the flux-based staggered grid representation often used in finite difference approaches. Two preconditioned conjugate gradient solvers are provided to efficiently solve the Poisson equation derived from the numerical formulation. The performance of these iterative solvers is further enhanced by the addition of a small, block diagonal stabilization ma-

trix to the Poisson equation matrix.

7. ATMOSPHERIC STABILITY PARAMETERIZATION

The primary method for incorporating atmospheric stability effects in ADAPT is by selection of the ratio of the Gauss precision moduli, $\alpha = \alpha_H / \alpha_V$, which controls the degree of adjustment in the vertical versus the horizontal wind components. Small values of α inhibit vertical velocity changes and are appropriate for stable flows, forcing steering around hills, while larger values of the parameter produce unstable flows and increase the likelihood of winds rising over topographic barriers.

For situations involving complex topography and spatially varying atmospheric stability, it is appropriate to let α vary over the entire domain. Our approach (Chan and Sugiyama, 1997b) is a modification of the Strouhal number parameterization proposed by Ross et al. (1988) and developed further by Moussiopoulos et al. (1988). An improved curve-fitting formula for α^2 as a function of local Strouhal number has been devised along with a generalized formula for determining a characteristic height difference to incorporate topographic effects.

The local Strouhal number is defined as

$$\text{Str} = \frac{H N}{U}, \quad N = \sqrt{\frac{g}{\theta} \frac{d\theta}{dz}}, \quad \frac{d\theta}{dz} \geq 0$$

$$\text{Str} = -\frac{H}{U t}, \quad t = \sqrt{-\frac{g}{\theta} \frac{d\theta}{dz}}, \quad \frac{d\theta}{dz} < 0 \quad (4)$$

where H is the characteristic height difference, N is the Brunt-Väisälä frequency, U is the characteristic wind speed, t is the buoyancy time scale, and θ is the potential temperature of the atmosphere. The characteristic wind speed is taken to be

$$U = \max(\sqrt{(u^o)^2 + (v^o)^2}, 0.2 \text{ m/s}) \quad (5)$$

For H , we use an inverse-distance weighting of the varying topographic height differences combined with a constant term involving the difference between the maximum and minimum terrain heights

$$H = c(h_{\max} - h_{\min}) + (1 - c) \frac{\sum_{i,j} |\Delta h_{ij}| / r_{ij}}{\sum_{i,j} 1 / r_{ij}} \quad (6)$$

where Δh_{ij} and r_{ij} are the orographic height difference and the horizontal distance between the considered location for H and location (i, j) on the terrain grid and h_{\max} and h_{\min} are the maximum and minimum terrain heights, respectively. The input parameter c varies between zero

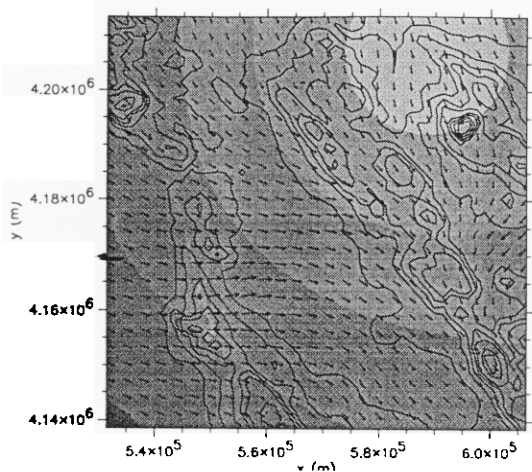


Figure 4: San Francisco Bay area winds and temperature (shaded contours) at 10 m AGL.

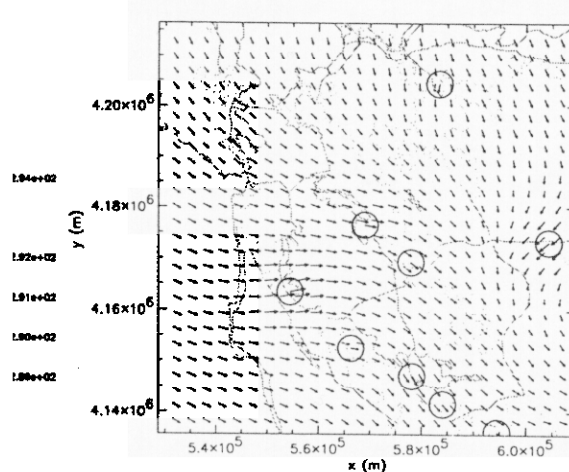


Figure 5: San Francisco Bay area winds and at 10 m AGL. The vectors enclosed by circle are the observational data.

and one and is used to select an appropriate linear combination of the two terms. The constant term allows treatment of flows characterized by a constant Strouhal number.

An exponential relationship between α^2 and the local Strouhal number was adopted

$$\alpha^2 = \begin{cases} \exp(-1.5\text{Str}^{1.5}) & \text{Str} \geq 0 \\ \exp(1.5(-\text{Str})^{1.5}) & \text{Str} < 0 \end{cases} \quad (7)$$

based on a curve fit to the experimental data of Hunt and Snyder (1980). The magnitude of the Strouhal number is capped between $[-3, 3]$ to prevent extreme values of α .

8. EXAMPLE : SAN FRANCISCO BAY

The Strouhal number parameterization of α was tested on the analytic hill problem studied by Hunt and Snyder (1980) with satisfactory results. A preliminary test using real data was performed for the San Francisco Bay area. Temperature and pressure fields interpolated from AVN global model data were combined to produce potential temperatures. The latter were used to develop the three-dimensional α field. Interpolated wind fields derived from a combination of forty local observations and AVN data were then adjusted for mass-consistency.

The grid covers a region 75 km square with 51 horizontal grid points. The grid top is at 3 km, with 31 vertical grid points and a finest resolution of 10 m near the ground. The 0Z March 29, 1997 temperatures and mass-consistent wind field for the 10 m AGL level are shown in Figures 4 and 5 along with the observational data. Figure 6 shows temperatures and winds at the $\sigma_z = 0.157$

or $z \approx 475$ m levels. The temperature increases inland, with generally onshore winds, veering to the south near the surface. Figure 7 plots a vertical cross-section through the center of the grid to show the w component generated by the mass-adjustment procedure.

9. CONCLUSION

ADAPT simulations have been performed to test the numerics, robustness, and computational efficiency of the model. Evaluation of ADAPT in conjunction with the new ARAC dispersion model (Leone et al., 1997) are underway using a variety of archived tracer experiment data. Initial comparisons with the current ARAC operational models (ARAC, 1997) indicate that ADAPT provides significantly improved winds as reflected in the arrival time, speed, and direction of the plume (Foster, 1997). An important factor in the improvement is the use of a continuous terrain representation and variable gridding, which allows meteorological features and topography to be more accurately resolved. An initial operational version is currently undergoing testing by ARAC.

Work has begun to refine the treatment of meteorological data, improve atmospheric parameterizations, incorporate momentum as well as mass conservation, and develop eddy diffusivities for dispersion calculations. Additional assimilation methods are also being implemented including three-dimensional analyses and approaches to combining analysis and forecast data with observations.

ACKNOWLEDGEMENTS

The authors would like to acknowledge H. Walker for

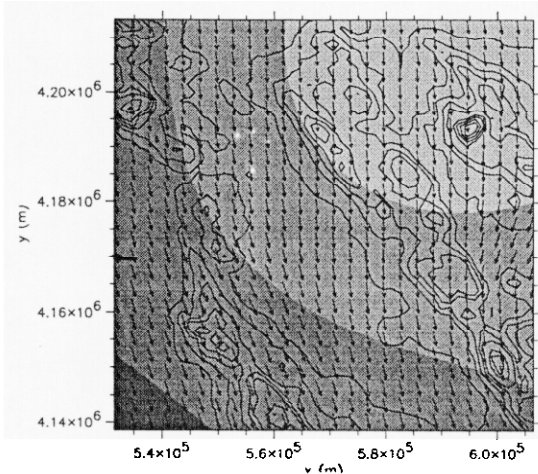


Figure 6: San Francisco Bay area winds and temperatures (shaded contours) at $\sigma_z = 0.157$ where $z_{top} = 3000$ m.

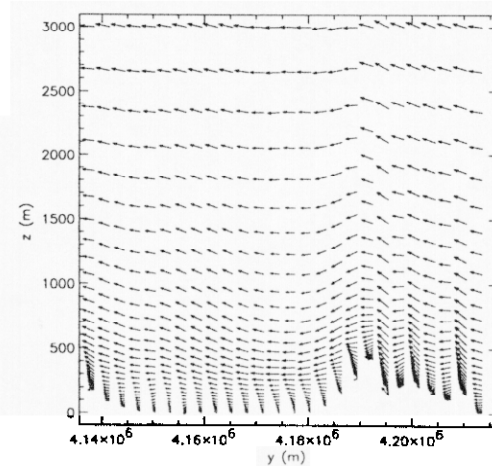


Figure 7: San Francisco Bay area winds at a vertical cross-section at $x = 569$ km. The vertical wind component is exaggerated by a factor of ten.

providing the grid generation model and T. Kuczmariski for the graphics package. This work was performed under the auspices of the U.S. Department of Energy by Lawrence Livermore National Laboratory under Contract No. W-7405-ENG-48.

REFERENCES

Atmospheric Release Advisory Capability, 1997: User's Guide to the CG-MATHEW/ADPIC Models, Version 5.0, UCRL-MA-103581 Rev. 5, Lawrence Livermore National Laboratory, Livermore, CA.

Chan, S. T. and G. Sugiyama, 1997a: A New Model for Generating Mass-Consistent Wind Fields over Continuous Terrain, *Proc. of the ANS Sixth Topical Meeting on Emergency Preparedness and Emergency Response, San Francisco, CA*, 375-378.

Chan, S. T. and G. Sugiyama, 1997b: User's Manual for MC_WIND: A New Mass-Consistent Wind Model for ARAC-3. (in preparation)

Daley, R., 1991: *Atmospheric Data Analysis*, Cambridge University Press, Cambridge, UK, and references cited therein.

Hodur, R. M., 1987: Evaluation of a Regional Model with an Update Cycle, *Mon. Wea. Rev.*, **117**, 2707.

Hodur, R. M. 1997: The Naval Research Laboratory's Coupled Ocean/Atmosphere Mesoscale Prediction System (COAMPS), *Mon. Wea. Rev.*, **125**, 1414-1430.

Hunt, J. C. R. and W. H. Snyder, 1980: Experiments on Stably and Neutrally Stratified Flow over a Model Three-Dimensional Hill, *J. Fluid Mech.*, **96**, Part 4, 671-704.

Foster, K., 1997: private communication.

Leone Jr., J. M., J. Nasstrom, and D. Maddix, 1997: A First Look at the New ARAC Dispersion Model, *Proc. of the ANS Sixth Topical Meeting on Emergency Preparedness and Emergency Response, San Francisco, CA*, 383-386.

Moussiopoulos, N. and Th. Flassak, and G. Knittel, 1988: A Refined Diagnostic Wind Model *Envir. Software*, **3**, No.2, 85-94.

Ross, D. G., and I. N. Smith, P. C. Manins, and D. G. Fox, 1988: Diagnostic Wind Field Modeling for Complex Terrain: Model Development and Testing, *J. Appl. Meteor.*, **27**, 785-796.